

# **Future Prediction of Scenario Based Land Use Land Cover (LU&LC)** **using DynaCLUE Model for a River Basin**

Kotapati Narayana Loukika <sup>1</sup>, Venkata Reddy Keesara <sup>2</sup>, Eswar Sai Buri <sup>1</sup>, Venkataramana Sridhar<sup>3\*</sup>

<sup>1</sup>Research Scholar, Department of Civil Engineering, National Institute of Technology Warangal, Telangana - 506004, India

<sup>2</sup>Professor, Department of Civil Engineering, National Institute of Technology Warangal, Telangana - 506004, India

<sup>3</sup>Professor, Department of Biological Systems Engineering, Virginia Polytechnic Institute and State University, Blacksburg, VA 24061, USA.

## **Abstract**

Human activities that cause changes to the surface of the Earth lead to alterations in Land Use and Land Cover (LU&LC) which have an impact on biodiversity, ecosystem functioning, and the well-being of humans. In order to comprehend and manage the effects of human activities on the environment, prediction of scenario-based LU&LC in future periods are crucial. Scenario-based predictions of LU&LC provide valuable insights for decision-makers in the sustainable governance of land and water resources. In the present study, the Dynamic Conversion of Land Use and its Effects (DynaCLUE) modelling platform was used to predict future LU&LC for Munneru river basin, India. Using six different user defined scenarios LU&LC change patterns were analysed in 2030, 2050 and 2080 so as to understand the pressure on the natural resources and to plan sustainable Land Use Planning by preserving the important land use classes. The connection between LU&LC classes and input driving factors was quantified using Binary Logistic Regression (BLR) analysis. The  $\beta$ -coefficient was estimated using LU&LC type as a dependent variable and driving factors as independent variables. The demands of each LU&LC type, spatial policies and constraints, characteristics of each location and land use conversions are used as inputs for prediction of future LU&LC maps. Major conversions in LU&LC observed in this basin from last two decades are the rapid increase in built-up area due to urbanization in the outskirts of cities and towns. The major LU&LC changes projected for the period of 2019–2080 are expansion of built-up area ranging from 42.5% to 88.5%, and a reduction in barren land ranging from 57.3% to 74.5% across all six scenarios in the entire basin. The projected LU&LC maps under different scenarios provide valuable insights that could aid local communities, government agencies, and stakeholders in systematically allocating resources at the local level and in preparing the policies for long-term benefits.

*Keywords: Land use change; Binary Logistic Regression; Driving Factors; DynaCLUE model; Prediction and Scenario; River basin management.*

## 33 **1.0 Introduction**

34 Changes in LU&LC can have negative effects on the functioning of ecological systems  
35 and also effect the natural processes of the environment (Le at al., 2008, Alonso et al., 2022).  
36 Understanding the potential evolution of land use is necessary since human actions greatly  
37 influence the distribution of land-cover. Anthropogenic impacts have drastically influenced the  
38 way that land is used, and as time goes on, its impact on the environment will have a significant  
39 effect on the utilization of land in the future (Sahoo et al., 2018). The LU&LC statistics in the  
40 past decades have shown the major land cover conversions such as agricultural land is  
41 converted to barren land, built-up and waterbodies, forest to barren land, waterbodies and  
42 cropland and other such changes (Hoekema and Sridhar, 2011; Meng et al., 2021, Behera et  
43 al., 2018). Due to the intricate and uncertain nature of land use dynamics, modelling the  
44 dynamics of change in LU&LC is a crucial aspect of studies related to LU&LC planning,  
45 impact on environmental assessment, and evaluation of policies for a specific region (Sujatha  
46 and Sridhar, 2021). Development of LU&LC scenarios has become more popular as it provides  
47 the possible conversions under anthropogenic and ecological processes in future circumstances  
48 (Schirpke et al., 2012, Sleeter et al., 2012, Ghadirian et al., 2023).

49 Studies have been carried out in numerous locations about the factors causing  
50 spatiotemporal changes in LU&LC in a particular area (Luwa et al., 2020; Duraisamy et al.,  
51 2018; Dibaba et al., 2020; Buaraka et al., 2022). Numerous studies have focused on particular  
52 LU&LC change processes where a single conversion, such as urbanization or deforestation, is  
53 dominant (Verburg and Overmars, 2009). To identify the causative factors of these changes  
54 and determine the regions where they are most prevalent, several LU&LC models are created  
55 and used (Wang et al., 2020; Jazouli et al., 2019; Venkatesh et al., 2020; Varanou, 2003;  
56 Waiyasusri et al., 2022). To help planners make more enlightened decisions and maintain a  
57 balance between urbanization and conservation of the environment, models that combine and  
58 assess many elements of LU&LC change can be utilized.

59 In recent years, several studies have utilized different models to predict Land Use and  
60 Land Cover (LU&LC) scenarios, such as Cellular Automata (CA)-Markov models and  
61 historical LU&LC change trend patterns (Behera et al., 2012; Tadese et al., 2021; Karimi et  
62 al., 2018; Tong et al., 2012; Loukika et al., 2022). Yao et al. (2023) studied spatiotemporal  
63 fluctuations in LU&LC and their effects on water quality in a river flowing through a rapidly  
64 developing area in China and LU&LC maps were predicted using CA-Markov model.  
65 Okwuashi et al. (2021) carried out the integration of Support Vector Machine (SVM), cellular

66 automata and Markov chain for urban land use change modelling over Lagos, Nigeria. They  
67 concluded that the inability of cellular automata to include driving forces of urban growth is  
68 achieved with the integration of SVM to determine the impact of the explanatory variables that  
69 drive change in the urban areas. They used the Markov chain to determine the urban transition  
70 probabilities between the various time periods. The Dynamics of Land System (DLS) model  
71 was also utilized in Najmuddin et al. (2007) to simulate LU&LC changes for the years 2020  
72 and 2030 in the Kabul River Basin (KRB), Afghanistan. The study found significant changes  
73 in land use, indicating the importance of understanding the underlying processes driving  
74 LU&LC change. Rong et al. (2022) created a land use carbon emission grid, and predicted  
75 future land use patterns in China under several scenarios from 2000 to 2018. Mitra et al. (2023)  
76 evaluated the influence of several LU&LC and climate scenarios on runoff in Kansabati river  
77 basin and LU&LC maps were predicted using IDRISI Land Change Modeller (LCM).

78 For simulating scenario-based LU&LC maps and understanding the spatial pattern in  
79 each location, studying the driving factors is crucial. The DynaCLUE modelling framework,  
80 which combines dynamic modelling with empirically measured relationships between land use  
81 and its driving elements, has been used in various research studies to simulate LU&LC change  
82 (Verburg et al., 1999).Adhikari et al. (2020) used the DynaCLUE model to predict LU&LC  
83 evolution in Vietnam by 2100 for a groundwater recharge study. Tizora et al. (2018) used the  
84 DynaCLUE model to simulate LU&LC changes in the Western Cape Province, South Africa,  
85 and suggested that the model can assist in future land use planning by considering policies that  
86 shape land use. Sahoo et al. (2018) simulated Land Use Suitability Zone (LSZ) mapping for  
87 future scenarios for agricultural sustainability using DynaCLUE for Dwarakeswar-  
88 Gandheswari river basin, India. Similarly, Das et al. (2019) used the DynaCLUE model for  
89 evaluating the growth and conversion to urban areas from rural areas in 2025 for the river basin  
90 of Mahanadi in India. The Dyna-CLUE model was used to study changes in the LU&LC  
91 pattern between 1975 and 2010 in order to gain a better understanding of the conversion process  
92 and predicted the future trend in LU&LC for the year 2045 (Behera et al., 2020). Roy et al.  
93 (2021) assessed future flood susceptibility in Ajoy river basin, India, with simulated LU&LC  
94 scenarios using pixel-wise association properties with the DynaCLUE model.

95 Loukika et al. (2022) reported that the CA Markov model did not detect any significant  
96 changes in future predicted LU&LC maps for the Munneru river basin in India. However, there  
97 have been no prior studies analyzing future LU&LC patterns in the basin under different user  
98 defined scenarios. The availability of remotely sensed data is very meagre before the year 2000.

99 So, we may not able to get the LU&LC maps with high resolution for that years. We are more  
100 interested to predict the LU&LC maps based on the user defined scenarios for the next 20 years  
101 to prepare the sustainable land use plans. We are also concerned about combined impact of  
102 climate and LU&LC change in long term basis for the next 60 years in the basin as most of the  
103 climate models provide projected data for 100 years. So we analysed LU&LC maps in 2030,  
104 2050 and 2080. Even though it will not exactly resemble the LULC changes in future years as  
105 per the climate change scenarios. Hence, we took user defined scenarios to get idea of how  
106 LULC change is occurring in the future periods. Therefore, this study presents predictions of  
107 future LU&LC maps for 2030, 2050, and 2080 years using the DynaCLUE model under  
108 various user-defined scenarios using 20 years of the past LU&LC maps. The LU&LC  
109 prediction was performed for six scenarios out of which two scenarios were predicted based on  
110 the past trend and remaining four scenarios were based on the restricted/unrestricted conditions  
111 of forest deforestation. These predictions can be beneficial for developing basin level  
112 watershed management policies in the long-term. The present analysis will assist researchers  
113 and policymakers in obtaining better land management practises, which will ultimately aid in  
114 the achievement of the Sustainable Development Goals (SDG's) (<https://sdgs.un.org/goals>).

## 115 **2.0 Study Area**

116 The Munneru River originates from the left tributary of the River Krishna and is located  
117 in the Lower side of the Krishna River basin, India which is also an independent sub-basin.  
118 The study area, as shown in Figure 1, is mostly an agriculture-dominated basin, covering a total  
119 area of 10,392 Km<sup>2</sup> across the Andhra Pradesh and Telangana states. The Munneru River basin  
120 lies between 16.6° N - 18.1° N (Latitudes) and 79.2° E - 80.8° E (Longitudes) (Loukika et al.,  
121 2021). The elevation of the basin ranges between 21m to 792m. The average annual rainfall  
122 for 119 years (1901-2022) is 1014 mm for the basin. Pakhal Lake, Wyra reservoir, Bhayyaram  
123 Cheruvu, and Lanka Sagar reservoir are the four major waterbodies in this basin. Red and black  
124 soils are the two most common types of soil in this basin. Khammam, along with adjacent areas  
125 like Dornakal and Mahabubabad, receives excessive rainfall, which frequently produces  
126 flooding on Munneru. According to 2011 census, the population present in the basin is  
127 32,11,441. The major crops grown in the basin are paddy, cotton, maize and chillies. The study  
128 area comprises of five primary types of LU&LC, namely, agricultural lands (72%), built-up  
129 (4%) areas, waterbodies (5%), forest areas (13%) and barren lands (6%). The major changes  
130 observed in the LU&LC maps during the time period from 2005 to 2019 in the urban areas of  
131 Khammam and Nandigama were the conversion of barren lands to built-up land. However, no

132 significant changes were observed in the remaining LU&LC types, such as agricultural land,  
133 forest area, and waterbodies. Rapid urbanization is taking place in some of the cities such as  
134 Khammam and Mahabubabad in the newly formed Telangana state. Whereas in Andhra  
135 Pradesh state, the new capital city named Amaravati which is near to the basin has the effect  
136 of increased urbanization in Nandigama which can cause tremendous impact on the water  
137 resources of the basin. As per the observed data, the basin contains sufficient water resources.  
138 The climate and LU&LC change in future periods may cause pressure on water distribution to  
139 different sectors. There is a need to study the scenarios of LU&LC change and to prepare the  
140 policies so that issues related water and environment can overcome.

141

### 142 **3.0 Data and Methods**

143 The methodology for predicting future scenario based LU&LC maps was outlined in  
144 Figure 2. The LU&LC maps obtained from Landsat 5 and 8 images were classified, and driving  
145 factors were selected based on existing literature. Binary Logistic Regression (BLR) analysis  
146 was performed to determine the efficient drivers, considering the driving factors and the  
147 classified LU&LC maps. The input parameters required for the Dyna CLUE model were  
148 prepared based on the BLR analysis, which falls under the non-spatial module. The model was  
149 compiled using all the input parameters, calibrated, and validated with the classified map of  
150 LU&LC. The future LU&LC maps were predicted under various scenarios, after the validation  
151 of the model. The steps of the methodology are thoroughly explained in the following sections.

#### 152 ***3.1 Preparation of LU&LC maps and Driving factors***

153 The LU&LC maps for 2005, 2010, 2015, and 2019 were created using Google Earth  
154 Engine, as described by Loukika et al. (2021). The driving factors used to project LU&LC  
155 maps under various scenarios included distance to road network, waterbodies, and buildings,  
156 as well as elevation, lineament density, population density, slope, and precipitation. These  
157 driving factors are illustrated in Figures 3 and 4 for the current study.

158 The layers of driving factors were generated using the GIS platform by combining data  
159 from various sources. The building and road network layers were obtained from an open-source  
160 website, DIVAGIS (<https://www.diva-gis.org/Data>). The waterbody layer was extracted from  
161 the 2015 LU&LC map in ArcGIS 10.5 Version. The distance to each stream and road network  
162 was calculated using Euclidean distance tool, determining the Euclidean distance between the  
163 centres of the source cells and each neighbouring cell. The Bhukosh website was used to extract

164 the lineament features (<https://bhukosh.gsi.gov.in>), and a spatial map was generated using the  
 165 kriging interpolation algorithm. A Digital Elevation Model (DEM) layer was created using  
 166 satellite data (CARTOSAT) which is downloaded from Bhuvan-NRSC website  
 167 (<https://bhuvan-app3.nrsc.gov.in/data/download/index.php>) with a resolution of 30 meters,  
 168 which was used to generate a slope map. Daily precipitation with a resolution of  $0.25^\circ \times 0.25^\circ$   
 169 was obtained from IMD gridded dataset  
 170 ([https://www.imdpune.gov.in/Clim\\_Pred\\_LRF\\_New/Gridded\\_Data\\_Download.html](https://www.imdpune.gov.in/Clim_Pred_LRF_New/Gridded_Data_Download.html)) to avail  
 171 the average annual precipitation. The Kriging interpolation technique was used to prepare the  
 172 precipitation raster layer using gridded precipitation data. The map related to population  
 173 density was created using global population data taken from the world population website  
 174 (<https://www.worldpop.org>). To maintain uniform projection and cell size with respect to land  
 175 use classes, the resultant spatial maps were re-projected and rescaled.

### 176 **3.2 DynaCLUE**

177 The CLUE modelling framework was constituted by the Institute for Environmental  
 178 Studies (IVM - <http://www.ivm.vu.nl>) (Das et al., 2019). CLUE uses dynamic modelling and  
 179 empirically defined relationships between LU&LC and driving forces to simulate changes in  
 180 land use. DynaCLUE is an improved version of the CLUE model (Verburg and Overmars,  
 181 2009; Castella and Verburg, 2007) that allocates spatial demand for various land use categories  
 182 to individual grid cells. DynaCLUE model version 2.0 has two components: spatial and non-  
 183 spatial. The spatial component contains geospatial layers, including the LU&LC map and  
 184 drivers, to examine the impacts of spatial factors on land use change. The data and model  
 185 parameters were defined in the main parameter file, which is part of the non-spatial module. In  
 186 the non-spatial component, the land use class requirements for the simulation year are stored,  
 187 while the allocation file captures the correlation between drivers and LU&LC and is used to  
 188 compute the suitability of each land cover in a specific location. The preference of location for  
 189 a particular land use type was determined using the logit model (Verburg, 2010) as illustrated  
 190 below.

$$191 \quad \text{Log}\left(\frac{P_i}{1-P_i}\right) = \beta_0 + \beta_1 X_{1,i} + \dots + \beta_n X_{n,i} \dots \dots \dots (1)$$

192 The probability of a specific land use type appearing in a grid cell located at  $i$  is represented  
 193 by  $P_i$ . The driving factor that affects the land use type is represented by  $X$ . The  $\beta$  coefficients  
 194 were determined through logistic regression, with the actual land use class serving as the  
 195 dependent variable.

### 196 **3.3 Binary Logistic Regression (BLR) Analysis**

197 The relationship between LU&LC classes and their determining factors and the  
198 suitability of each land cover class for every factor, was analyzed using BLR. When conducting  
199 statistical analysis on a binary outcome variable, which takes on only two possible values  
200 (usually 0 and 1), binary logistic regression is a commonly used method. This method is  
201 applicable regardless of whether the independent variables used in the analysis are continuous  
202 or categorical.

203 The compatibility between different types of LU&LC at the cell level is established  
204 according to the suitability of a particular location. This suitability is determined by a weighted  
205 average method, which is calculated through empirical analysis that reflects current and  
206 historical preferences for location based on specific characteristics of the location (Verburg et  
207 al., 2008). The location preferences of different LU&LC classes can be understood by  
208 performing BLR model. The model established connections between each of the land use class  
209 and potential driving factors that drive their location preferences. The influence of each driver  
210 on a particular LU&LC can be effectively interpreted using the odds ratio  $\left(\frac{P_i}{1-P_i}\right)$  generally  
211 referred as  $\text{Exp}(\beta)$ . The probability of a grid cell being assigned to a particular LU&LC class  
212 in a specific location is denoted as  $P_i$ . The odds ratio is a measure of how a change in the  
213 independent variable by one unit, while holding all other factors constant, impacts the occurring  
214 of dependent variable's probability. If the exponential of  $\beta$  is greater than 1, then an increase  
215 in the independent variable will lead to an increase in the probability. Conversely, if  $\text{Exp}(\beta)$  is  
216 less than 1, the probability will decrease (Overmars and Verburg, 2005).

### 217 **3.4 Input parameters for the DynaCLUE**

218 The parameters used in the non-spatial module and the spatial module creates a set of  
219 scenarios and possible outcomes which are utilised by the model for prediction of LU&LC.

#### 220 **3.4.1 Conversion matrix**

221 The conversion of one land cover to another is determined by the conversion matrix,  
222 which defines whether such conversions are restricted or allowed. The conversion matrix  
223 assigns binary values of 1 and 0 to represent allowed and restricted conversion types,  
224 respectively. In the matrix, a value of 1 would indicate that a particular conversion is permitted.  
225 Conversely, if the reverse conversion is not permitted, the value assigned to it would be 0.

#### 226 3.4.2 Conversion elasticity

227 Conversion elasticity is a parameter included in the main file that indicates how flexible  
228 the conversion process of land cover is. The accuracy of simulation between estimated and  
229 demand area is defined in convergence criteria. The main file includes information such as the  
230 beginning and finishing years of the simulation, number of iterations, number of LU&LC types  
231 and the size of the cells. The range of conversion elasticity values is 0 to 1. Therefore, lower  
232 conversion likelihoods will occur with larger values and values close to 0 indicate higher  
233 conversion possibilities. Built-up areas are assigned a conversion elasticity value of 1 (for no  
234 conversion), while forest, agricultural land, and waterbodies have values of 0.8, 0.7, and 0.7,  
235 respectively. Barren land has a conversion elasticity value of 0.4.

#### 236 3.4.3 Convergence Criteria

237 Convergence criteria is a measure used to determine whether the actual and model-  
238 simulated LU&LC areas match. To define convergence criteria, three variables must be  
239 specified: iteration mode, first convergence criteria, and second convergence criteria. The  
240 iteration mode options are 0 or 1, with 0 indicating criteria in percentage of demand and 1 for  
241 absolute values. The average deviation between actually allocated changes and demand  
242 changes is the first convergence criterion, and the second convergence criteria is the largest  
243 deviation among actually allocated changes and demand changes.

244 For the present study, the lower limit of the convergence criteria was set at an average  
245 and maximum allowable difference of 5 and 18, respectively. To improve the model's  
246 prediction accuracy, the conversion elasticity and convergence criteria were repeatedly  
247 evaluated. The change matrix was developed by taking into account the long-term changes in  
248 LU&LC over the course of a decade, as well as the level of understanding of the interpreter.  
249 The simulation model was highly complex and could only function properly with convergence  
250 values above a certain threshold. However, setting the maximum convergence value too high  
251 could result in inaccurate predictions for certain classes.

#### 252 3.4.4 Demand Estimation

253 Land-use demands pertain to the anticipated pattern of land use classes within a specific  
254 research area over time. The estimation of land-use demand involves creating a continuous  
255 dataset of aggregate land use classes. There are several methods for estimating demand,  
256 including linear extrapolation of system dynamics, socioeconomic models, and historical

257 trends. In this study, linear interpolation is used as the method for estimating demand. This  
258 involves calculating the aggregated land use changes by extrapolating from the land use details  
259 at two time extremes and determining the demand for the years in between. The demand was  
260 generated by using linear interpolation and extrapolation techniques for intermediate and future  
261 years with the classified LU&LC's of 2005, 2010, 2015 and 2019.

### 262 *3.5 LU&LC Scenarios*

263 Based on the land use and land cover (LU&LC) maps from previous years, six different  
264 user-defined scenarios were considered for projecting future LU&LC maps, as shown in Table  
265 1. The BLR analysis results and the input parameters were fed into the model for the prediction  
266 of the LU&LC maps. For Scenario 1, the transitions in LU&LC observed during the period  
267 2005-2015 were used to predict maps of LU&LC for 2030, 2050, and 2080. The trend observed  
268 during the period 2010-2019 was utilised to predict LU&LC maps for the years 2030, 2050,  
269 and 2080 in scenario 2. The model projections were carried out under two different demand  
270 conditions: the first set included scenarios with less changes (Scenario 3) and moderate changes  
271 with restricted deforestation (Scenario 4), while the second set included scenarios with less  
272 changes (Scenario 5) and moderate changes without forest preservation (unrestricted  
273 deforestation) (Scenario 6).

274 The scenarios were formulated by considering historical patterns observed in the basin  
275 and utilized to forecast future demands under conditions of restricted and unrestricted  
276 deforestation. The 2005 LU&LC map was used as base map and 2019 map was simulated and  
277 validated with 2019 classified map. Subsequently, the 2019 map was used as the initial map  
278 for future simulations. The third and fourth scenarios were considered based on the observed  
279 trend, which suggests that agricultural and built-up areas will continue to expand over time  
280 without disturbing the ecological balance by restricting the changes in forest area. The extent  
281 of this increase was determined by averaging historical changes, resulting in a minimum annual  
282 increase of 2 Km<sup>2</sup> and a maximum annual increase of 6 Km<sup>2</sup> in the built-up area. The fifth and  
283 sixth scenarios were formulated assuming unrestricted deforestation, resulting in a reduction  
284 of forested areas and corresponding increases in agriculture, built-up areas, and barren land. In  
285 addition to the aforementioned expansion of built-up areas, the agricultural area is expected to  
286 experience a minimum annual increase of 10 Km<sup>2</sup> and a maximum annual increase of 20 Km<sup>2</sup>.  
287 The driving factors were taken into account to determine the probability of transitioning to a  
288 specific land use and land cover (LU&LC) class. Based on these driving factors, future

289 demands specified in DynaCLUE were assigned to regions where there is a likelihood of  
290 transitioning to a different LU&LC class.

## 291 **4.0 Results and Discussions**

### 292 *4.1 BLR Analysis*

293 The logistic regression-derived  $\beta$ -coefficients are presented in Table 2, showing the  
294 odds ratio of driving factors influencing land use. Lineament and precipitation have a positive  
295 impact on water body conversion. A high lineament density indicates a lack of hard rock, which  
296 reduces the likelihood of water body conversion into other irreplaceable land uses. Conversely,  
297 a high lineament density provides a free-flowing passage, thereby increasing the chances of  
298 water body transition. Increased precipitation increases water body storage capacity, reducing  
299 the likelihood of conversion to other land use classes. The slope and population density are  
300 negatively correlated with water body land use. This indicates that water body occurrence  
301 decreases with increasing vertical altitude and steepness, and increasing population density  
302 increases dependency on water bodies, leading to a reduction in water percentage and a  
303 negative correlation with population density. The slope, precipitation, and distance to water  
304 bodies have a positive relationship with forest land. Forest occurrence increases with steepness,  
305 and precipitation contributes to forest growth.

306 In the Munneru river basin, agricultural land usage is predominantly found on flat  
307 terrain close to streams, as demonstrated by the inverse correlation between distance to water  
308 bodies, slope, and distance to roads. In contrast, precipitation and lineament density show a  
309 positive relation with agricultural lands, as an increase in these factors contributes to water  
310 storage and passage in the surface and subsurface, leading to an increment of farmlands. Urban  
311 area expansion, on the other hand, is primarily attributed to the rise in population density in  
312 various regions of the study area, as indicated by the strongest positive factor contributing to  
313 the increase in urban area being population density, followed by distance to road driver.  
314 Distance to water body projects a positive relation with barren land, as the distance between  
315 cultivated lands or agricultural land to water body increases, the chances of irrigation reduce,  
316 thereby leaving the land barren.

317 To study the spatial variation occurring in LU&LC types of the Munneru river basin,  
318 the results of the binary logistic regression model were analyzed. These results are then used  
319 as input for the Dyna CLUE model to simulate the changes that may occur in future years.  
320 Since not all the drivers may be influential, the drivers showing a significant value of less than  
321 0.01 are considered in the present study.

322 The Relative Operating Characteristic (ROC) is a statistical tool used to evaluate the  
323 goodness of fit for logistic regression. Figure 5 shows the ROC curves for the five LU&LC  
324 classes. The ROC value ranges from 0 to 1, with values closer to 1 indicating an excellent fit  
325 and 0.5 representing a random fit. Based on Figure 5, it can be observed that water bodies have  
326 a perfect fit, accompanied by forest area, built-up, agricultural land, and barren land.

#### 327 ***4.2 LU&LC Dynamics***

328 We divided the the study area into five major LU&LC classes including Built-up,  
329 waterbodies Agriculture, Forest and Barren land. The LU&LC maps of the years 2005, 2010,  
330 2015 and 2019 were presented in Figure 6. The classification accuracy was determined to be  
331 91.2%, 92.6%, 94.3% and 95%, respectively, with the kappa coefficients of 0.85, 0.91, 0.92  
332 and 0.93. The LU&LC statistics of the classified maps were summarized in Table 3.

333 Within the study area, the agricultural land was found to be dominant accounting for  
334 68.49% in 2005, 68.92% in 2010, 71.01% in 2015 and 71.96% in 2019. Forest was the second  
335 most common land cover with 13.63% in 2005, 13.63% in 2010, 13.57% in 2015 and 13.57%  
336 in 2019. Barren land decreased by 0.97% in 2010, 1.88% in 2015 and 0.99% in 2019 compared  
337 to the 2005 LU&LC map. There was little change observed in waterbodies, which covered  
338 5.35% of the area in 2005, 5.36% in 2010, 5.16% in 2015 and 5.16% in 2019. Barren land was  
339 found to be converting to built-up area, with an increase of 0.54% in 2010, 0.04% in 2015 and  
340 0.04% in 2019 compared to the 2005 LU&LC map. Overall, the study area's LU&LC statistics  
341 revealed a relative stability in the LU&LC patterns over the studied period.

#### 342 ***4.3 Predicted LU&LC maps under different scenarios***

343 The LU&LC maps for the Munneru river basin were projected under six different  
344 scenarios and plotted. Figure 7 displays the LU&LC maps for Scenario 1 and Scenario 2 for  
345 the projected years. A detailed explanation of each scenario was provided. Table 4 shows the  
346 percentages of LU&LC types for the respective years under various scenarios in the study area.

##### 347 ***4.3.1. Scenario 1***

348 The prediction of LU&LC for Scenario 1 follows the same trend as the previous period  
349 from 2005 to 2015. The predicted LU&LC map, when compared to 2019, shows that the built-  
350 up area will rise by 13.5% in 2030, 39.5% in 2050, and 59.5% in 2080. The reduction in barren  
351 land is expected to be 30.3% in 2030, 51.3% in 2050, and 66.2% in 2080. Agricultural land is  
352 projected to increase by 2.5% in 2030, 2.7% in 2050, and 3.3% in 2080. The forest area is not

353 expected to undergo significant change in future periods. However, the waterbodies are  
354 predicted to decrease by 3.7% in 2030, 6.6% in 2050, and 9.7% in 2080. The major changes in  
355 predicted LU&LC are an increase in built-up and agricultural land, followed by a reduction in  
356 barren land, forest, and waterbodies. From the results obtained from scenario1, there may be  
357 additional requirement of water in the basin due to extension of built-up and agricultural areas.  
358 The current policy should be revised for meeting the water demand due to increase in built  
359 upland and agriculture land.

#### 360 4.3.2. Scenario 2

361 In scenario 2, LU&LC map was predicted using the past trend of LU&LC during the  
362 period 2010-2019. The predicted LU&LC map under scenario 2 shows an expansion in built-  
363 up area and agricultural land, and a decrease in barren land, forest, and waterbodies. The  
364 predicted LU&LC map when compared to 2019 indicated rise in built-up area of 10.4% in  
365 2030, 19.6% in 2050, and 42.8% in 2080. It was observed that there was a reduction in barren  
366 land of 34.7% by 2030, 54.1% by 2050, and 68% by 2080. Agricultural land was increased by  
367 4.3% in 2030, 3.6% in 2050, and 4.3% in 2080. Similar study states that to simulate extreme  
368 agricultural area, system dynamics-based scenarios might be coupled with the CA model  
369 (Ghadirian et al., 2023). The forest area did not show any significant change in the future  
370 periods. The waterbodies area was decreased by 7.7% in 2030, 4.3% in 2050, and 8% in 2080.  
371 Scenario 2 showed the same trend patterns as scenario 1, but the percentage changes varied.  
372 As per the recommendations followed in scenario 1, more or less the same type of practical  
373 implications will be applied in the basin for scenario 2.

#### 374 4.3.3. Scenario 3

375 The LU&LC maps for Scenario 3 and Scenario 4 for projected years depicted in the  
376 Figure 8. Scenario 3 involved restricted deforestation and a limit of 2 km<sup>2</sup> per year for changes  
377 in built-up area. The predicted LU&LC map, when compared to the 2019 map, showed an  
378 increase in built-up area of 5.9% by 2030, 29.8% by 2050, and 49.1% by 2080. It was also  
379 observed that the barren land decreased by 16.5% by 2030, 45.6% by 2050, and 57.3% by  
380 2080. Agricultural land increased by 0.7% in 2030, 2.4% in 2050, and 2.6% in 2080. The forest  
381 area did not show any significant change during the study period. Waterbodies decreased by  
382 2.9% in 2050 and 5.9% in 2080. This scenario is proposed based on forest conservation policies  
383 and shifting of people to nearby cities (increase in urbanization). The major changes predicted

384 in LU&LC were increased built-up followed by a reduction in barren land. In 2080, the  
385 conversion of barren into urban-area is higher when compared to 2030 and 2050.

#### 386 4.3.4. Scenario 4

387 Scenario 4 involved restricted deforestation and a change in built-up area of 6 km<sup>2</sup> per  
388 year. The predicted LU&LC map indicated a growth in built-up area by 17.6% in 2030, 55.9%  
389 in 2050, and 88.6% in 2080 when compared to 2019. It was observed that the reduction in  
390 barren land was 30.1% by 2030, 51.8% by 2050, and 65.9% by 2080. Agricultural land was  
391 increased by 1.7% in 2030, 1.9% in 2050, and 1.1% in 2080. The forest area did not show any  
392 significant change in the future periods. Waterbodies decreased by 2.9% in 2030, 6.9% in 2050,  
393 and 4.3% in 2080. Higher rate of urbanization is the main assumption for formulating this  
394 scenario while the conversion of forest area to other LULC is restricted. Hence we need to  
395 optimize the resources like water and land according to the rate of growth in urbanization.

#### 396 4.3.5. Scenario 5

397 The LU&LC maps for Scenario 5 and Scenario 6 for projected years depicted in the  
398 Figure 9. In Scenario 5 involved unrestricted deforestation whereas, the built-up area was  
399 allowed to increase by 2 Km<sup>2</sup> and agricultural land by 10 Km<sup>2</sup> annually. The predicted LU&LC  
400 map showed an increased growth in built-up area by 4.7% in 2030, 29.8% in 2050, and 49.5%  
401 in 2080 compared to 2019. The scenario also resulted in a reduction in barren land by 20.8%  
402 in 2030, 39.1% in 2050, and 59.7% in 2080, while agricultural land increased by 2.2% in 2030,  
403 2.6% in 2050, and 4.7% in 2080. Forest area decreased by 3.5% in 2030, 3.1% in 2050, and  
404 11.3% in 2080, and waterbodies area decreased by 1.4% in 2030, 6.6% in 2050, and 5.0% in  
405 2080. The primary change observed in the predicted LU&LC was the increased built-up area,  
406 followed by a reduction in barren land, forest, and waterbodies. In this scenario, deforestation  
407 is permitted, resulting in an increase in built-up and agricultural areas. Therefore, it is essential  
408 to educate people on forest conservation policies to ensure that there is a balance in the  
409 ecosystem. Governments may pass laws that support reforestation, forest conservation and  
410 programmes for restoring the forest. Such measures can lessen deforestation, protect  
411 biodiversity, and lessen the effects of climate change.

#### 412 4.3.6. Scenario 6

413 The predicted LU&LC map in scenario 6, which involved unrestricted deforestation  
414 and moderate changes, led to a phenomenal built-up area growth when compared to 2019.

415 Specifically, there was an increase of 17.7% in 2030, 50.6% in 2050, and 88.5% in 2080. The  
416 reduction in barren land was also notable, with a decrease of 30.8% by 2030, 67.7% by 2050,  
417 and 74.5% by 2080. Agricultural land increased by 3.1% in 2030, 3.9% in 2050, and 5.8% in  
418 2080. However, forest area decreased by 7.5% in 2030, 5.1% in 2050, and 20.8% in 2080,  
419 while waterbodies decreased by 2.3% in 2030, 7.2% in 2050, and 7.1% in 2080. In the fifth  
420 scenario, deforestation of the forest is permitted with the aim of maximizing the expansion of  
421 built-up and agricultural areas. To ensure the effective preservation and protection of forest  
422 resources, it is necessary to implement awareness programs targeting the local populations.  
423 Governments can employ land use planning where it is most suited, such as those with already-  
424 existing infrastructure, easy access to transportation, and services. By doing so, urban sprawl  
425 and the conversion of forest land to built-up area can be lessened.

426 Comparing scenario 1 and scenario 2, there were no significant changes observed in the  
427 predicted LU&LC maps for 2030, 2050, and 2080. In scenario 4, which involved demand  
428 conditions and unrestricted deforestation, there was more expansion of agricultural and built-  
429 up area than in scenario 3. Specifically, the expansion of built-up area was 6 Km<sup>2</sup> per year. In  
430 scenario 5 and scenario 6, where there was an expansion in agricultural and built-up area of 20  
431 Km<sup>2</sup> and 6 Km<sup>2</sup> per year, respectively, similar trends were observed. As there was unrestricted  
432 deforestation and high changes in built-up area, scenario 6 exhibited a high percentage of surge  
433 in built-up area, a reduction of barren and forest land. In 2080, the decrease of forest land was  
434 9.5% more in scenario 6 than in scenario 5. Similarly, the percentage decrease of barren land  
435 was 14.8% more in scenario 6 compared to scenario 5. Overall, the change of barren land to  
436 built-up area exponentially increased from 2019 to 2080 under all six scenarios. This trend is  
437 in agreement with similar studies (Venkatesh et al., 2020; Das et al., 2019). However, unlike  
438 other studies where agricultural land and forest areas were frequently affected by a declining  
439 trend (Rimal et al., 2018; Li et al., 2020), agricultural land in the present study had a progressive  
440 growth, which was similar to other studies (Waiyasusri et al., 2022).

441 The determination of conversion elasticity in the CLUE model relies on the user's  
442 understanding of the situation, and the chosen value for conversion elasticity significantly  
443 impacts the resulting patterns of land use (Verburg et al., 2002). This is because conversion  
444 elasticity directly affects the paths of change and the historical patterns of land use. The  
445 inherent uncertainty in simulating land use change due to the subjective nature of conversion  
446 elasticity calls for the development of a more quantitative approach. It is essential to propose a  
447 new solution that utilizes existing historical land use data to better define and quantify

448 conversion elasticity (Luo et al., 2010). Furthermore, enhancing the calibration process of the  
449 CLUE model by improving the settings of model parameters becomes crucial in order to  
450 address this challenge effectively. However, it is suggested to apply the current methodology  
451 in other geographical regions to improve its efficiency. The results of this study using the  
452 DynaCLUE model are ideal for tracking alterations in LU&LC in a region. The model takes  
453 into account the key drivers evaluated within a specific scenario that align with the defined  
454 objectives. Consequently, the outcomes of each scenario offer optimal solutions for making  
455 informed decisions regarding systematic land-use planning in the study region.

## 456 **5.0 Conclusions**

457 The present study analyzed the future predicted LU&LC maps using the DynaCLUE  
458 model for the years 2030, 2050 and 2080 in the Munneru Basin, India, considering six different  
459 scenarios. To achieve this, the DynaCLUE model was first validated using the 2019 classified  
460 LU&LC map, and then used to predict future periods under different scenarios with user-  
461 defined demand conditions. The relationship between LU&LC and driving factors was  
462 established using binary logistic regression analysis. The results revealed that both barren land  
463 and forest area were transitioned into agricultural land and built-up area, with the maximum  
464 change observed from 2019 to 2030 in the form of decreasing barren land and minimal changes  
465 in the forest area. This trend was also observed for 2030 to 2050 and 2050 to 2080. Scenarios  
466 5 and 6, which involved unrestricted deforestation, exhibited greater changes in the forest area,  
467 leading to an increase in agricultural land. From 2019 to 2080, the maximum growth of built-  
468 up area and agricultural land was noticed in scenario 6, and the maximum reduction of barren  
469 land and forest land was also observed in this scenario. It was also noted that there was a drastic  
470 decrease in barren land in 2080, with half of the area getting converted to agriculture or built-  
471 up area. This is not unexpected as food security and dwelling concerns are looming to an extent  
472 in several parts of the world (Kang and Sridhar, 2021). To deal with future shortages of water,  
473 it is critical to optimize water utilization by building reservoirs and improving water usage  
474 efficiency productivity. Finally, population control and balanced socioeconomic development  
475 will aid in sustainable land use management. The model's results predict potential future  
476 variations in land use change. Rapid degradation of forest and water regions suggests that the  
477 government need to develop comprehensive land use planning to promote rational utilization  
478 of land resources. The proposed policies for sustainable land management obtained from  
479 scenario based LULC changes can be better implemented by involving the all the local  
480 stakeholders. The findings of this research have the potential to assist in the creation of policies

481 that promote sustainable land use management. Additionally, this study will analyze the effects  
482 of changes in LU&LC under various scenarios within the river basin, with the goal of  
483 developing a comprehensive model for integrated water resources management.

#### 484 **Acknowledgements**

485 The corresponding author's (V. Sridhar) effort was funded in part by the Virginia Agricultural  
486 Experiment Station (Blacksburg) and through the Hatch Program of the National Institute of  
487 Food and Agriculture at the United States Department of Agriculture (Washington, DC) and  
488 as a Fulbright- Nehru senior scholar funded by the United States India Educational Foundation.

489 **References**

- 490 Adhikari, R.K., Mohanasundaram, S. and Shrestha, S., 2020. Impacts of land-use changes on  
491 the groundwater recharge in the Ho Chi Minh city, Vietnam. *Environmental Research*, 185,  
492 p.109440.
- 493 Acuña-Alonso, C., Novo, A., Rodríguez, J.L., Varandas, S. and Álvarez, X., 2022. Modelling  
494 and evaluation of land use changes through satellite images in a multifunctional catchment:  
495 Social, economic and environmental implications. *Ecological Informatics*, 71, p.101777.
- 496 Behera, M.D., Borate, S.N., Panda, S.N., Behera, P.R. and Roy, P.S., 2012. Modelling and  
497 analyzing the watershed dynamics using Cellular Automata (CA)–Markov model–A geo-  
498 information based approach. *Journal of earth system science*, 121, pp.1011-1024.
- 499 Behera, N.K. and Behera, M.D., 2020. Predicting land use and land cover scenario in Indian  
500 national river basin: the Ganga. *Tropical Ecology*, 61, pp.51-64.
- 501 Buraka, T., Elias, E. and Lelago, A., 2021. Analysis and Prediction of Land Use/land Cover  
502 Changes and Driving Forces by Using GIS and Remote Sensing in the Coka Watershed,  
503 Southern Ethiopia.
- 504 Das, P., Behera, M.D., Pal, S., Chowdary, V.M., Behera, P.R. and Singh, T.P., 2019. Studying  
505 land use dynamics using decadal satellite images and DynaCLUE model in the Mahanadi River  
506 basin, India. *Environmental monitoring and assessment*, 191, pp.1-17.
- 507 Dibaba, W.T., Demissie, T.A. and Miegel, K., 2020. Drivers and implications of land use/land  
508 cover dynamics in Finchaa catchment, northwestern Ethiopia. *Land*, 9(4), p.113.
- 509 Duraisamy, V., Bendapudi, R. and Jadhav, A., 2018. Identifying hotspots in land use land cover  
510 change and the drivers in a semi-arid region of India. *Environmental monitoring and  
511 assessment*, 190(9), p.535.
- 512 El Jazouli, A., Barakat, A., Khellouk, R., Rais, J. and El Baghdadi, M., 2019. Remote sensing  
513 and GIS techniques for prediction of land use land cover change effects on soil erosion in the  
514 high basin of the Oum Er Rbia River (Morocco). *Remote Sensing Applications: Society and  
515 Environment*, 13, pp.361-374.
- 516 Ghadirian, O., Lotfi, A., Moradi, H., Boushehri, S.N.S. and Yousefpour, R., 2023. Area-based  
517 scenario development in land-use change modeling: A system dynamics-assisted approach for  
518 mixed agricultural-residential landscapes. *Ecological Informatics*, 76, p.102129.
- 519 Hoekema, D., Sridhar, V., 2011. Relating climatic attributes and water resources  
520 allocation: A study using surface water supply and soil moisture indices in the Snake River  
521 basin, Idaho, *Water Resources Research* 47 (7), W07536, doi: 10.1029/2010WR009697
- 522 Kang, H., Sridhar, V., Mainuddin, M., Trung, L.D., 2021. Future rice farming threatened by  
523 drought in the Lower Mekong Basin, *Nature Scientific Reports*, 11:9383, doi: 10.1038/s41598-  
524 021-88405-2.
- 525 Karimi, H., Jafarnezhad, J., Khaledi, J. and Ahmadi, P., 2018. Monitoring and prediction of  
526 land use/land cover changes using CA-Markov model: a case study of Ravansar County in Iran.  
527 *Arabian Journal of Geosciences*, 11, pp.1-9.

528 Kilama Luwa, J., Bamutaze, Y., Majaliwa Mwanjalolo, J.G., Waiswa, D., Pilesjö, P. and  
529 Mukengere, E.B., 2021. Impacts of land use and land cover change in response to different  
530 driving forces in Uganda: evidence from a review. *African Geographical Review*, 40(4),  
531 pp.378-394.

532 Le, Q.B., Park, S.J., Vlek, P.L. and Cremers, A.B., 2008. Land-Use Dynamic Simulator  
533 (LUDAS): A multi-agent system model for simulating spatio-temporal dynamics of coupled  
534 human–landscape system. I. Structure and theoretical specification. *Ecological Informatics*,  
535 3(2), pp.135-153.

536 Li, H. and Song, W., 2020. Pattern of spatial evolution of rural settlements in the Jizhou District  
537 of China during 1962–2030. *Applied Geography*, 122, p.102247.

538 Loukika, K.N., Keesara, V.R. and Sridhar, V., 2021. Analysis of land use and land cover using  
539 machine learning algorithms on google earth engine for Munneru River Basin, India.  
540 *Sustainability*, 13(24), p.13758.

541 Loukika, K.N., Keesara, V.R., Buri, E.S. and Sridhar, V., 2022. Predicting the Effects of Land  
542 Use Land Cover and Climate Change on Munneru River Basin Using CA-Markov and Soil and  
543 Water Assessment Tool. *Sustainability*, 14(9), p.5000.

544 Luo, G., Yin, C., Chen, X., Xu, W. and Lu, L., 2010. Combining system dynamic model and  
545 CLUE-S model to improve land use scenario analyses at regional scale: A case study of  
546 Sangong watershed in Xinjiang, China. *Ecological Complexity*, 7(2), pp.198-207.

547 Meng, Y., Yang, M., Liu, S., Mou, Y., Peng, C. and Zhou, X., 2021. Quantitative assessment  
548 of the importance of bio-physical drivers of land cover change based on a random forest  
549 method. *Ecological Informatics*, 61, p.101204.

550 Mitra, S.S., Kumar, A., Santra, A. and Routh, S., 2023. Investigating impact of CORDEX-  
551 based predicted climatic and LCM-based LULC scenarios on hydrologic response of a semi-  
552 gauged Indian catchment. *Environmental Monitoring and Assessment*, 195(4), p.450.

553 Okwuashi, O. and Ndehedehe, C.E., 2021. Integrating machine learning with Markov chain  
554 and cellular automata models for modelling urban land use change. *Remote Sensing  
555 Applications: Society and Environment*, 21, p.100461.

556 Rimal, B., Zhang, L., Keshtkar, H., Haack, B.N., Rijal, S. and Zhang, P., 2018. Land use/land  
557 cover dynamics and modeling of urban land expansion by the integration of cellular automata  
558 and markov chain. *ISPRS International Journal of Geo-Information*, 7(4), p.154.

559 Rong, T., Zhang, P., Zhu, H., Jiang, L., Li, Y. and Liu, Z., 2022. Spatial correlation evolution  
560 and prediction scenario of land use carbon emissions in China. *Ecological Informatics*, 71,  
561 p.101802.

562 Roy, P., Pal, S.C., Arabameri, A., Rezaie, F., Chakraborty, R., Chowdhuri, I., Saha, A., Malik,  
563 S. and Das, B., 2021. Climate and land use change induced future flood susceptibility  
564 assessment in a sub-tropical region of India. *Soft Computing*, 25, pp.5925-5949.

565 Sahoo, S., Sil, I., Dhar, A., Debsarkar, A., Das, P. and Kar, A., 2018. Future scenarios of land-  
566 use suitability modeling for agricultural sustainability in a river basin. *Journal of cleaner  
567 production*, 205, pp.313-328.

568 Schirpke, U., Leitinger, G., Tappeiner, U. and Tasser, E., 2012. SPA-LUCC: Developing land-  
569 use/cover scenarios in mountain landscapes. *Ecological Informatics*, 12, pp.68-76.

570 Sleeter, B.M., Sohl, T.L., Bouchard, M.A., Reker, R.R., Soulard, C.E., Acevedo, W., Griffith,  
571 G.E., Sleeter, R.R., Auch, R.F., Sayler, K.L. and Prisley, S., 2012. Scenarios of land use and  
572 land cover change in the conterminous United States: Utilizing the special report on emission  
573 scenarios at ecoregional scales. *Global Environmental Change*, 22(4), pp.896-914.

574 Sujatha, E.R., Sridhar, V., 2021. Landslide Susceptibility Analysis in the Era of Climate  
575 Change: A Logistic Regression Model Case Study in Coonoor, India, *Hydrology*, 8(1), 41, doi:  
576 10.3390/hydrology8010041.

577 Tadese, S., Soromessa, T. and Bekele, T., 2021. Analysis of the current and future prediction  
578 of land use/land cover change using remote sensing and the CA-markov model in Majang forest  
579 biosphere reserves of Gambella, southwestern Ethiopia. *The Scientific World Journal*, 2021,  
580 pp.1-18.

581 Tizora, P., Le Roux, A., Mans, G. and Cooper, A.K., 2018. Adapting the DynaCLUE model  
582 for simulating land use and land cover change in the Western Cape Province. *South African  
583 Journal of Geomatics*, 7(2), pp.190-203.

584 Tong, S.T., Sun, Y., Ranatunga, T., He, J. and Yang, Y.J., 2012. Predicting plausible impacts  
585 of sets of climate and land use change scenarios on water resources. *Applied Geography*, 32(2),  
586 pp.477-489.

587 Varanou, E., Pikounis, M., Baltas, E. and Mimikou, M., 2003. Application of the SWAT model  
588 for the sensitivity analysis of runoff to land use change. In 2003 International SWAT  
589 Conference (p. 89).

590 Verburg, P.H., Soepboer, W., Veldkamp, A., Limpiada, R., Espaldon, V. and Mastura, S.S.,  
591 2002. Modeling the spatial dynamics of regional land use: the CLUE-S model. *Environmental  
592 management*, 30, pp.391-405.

593 Verburg, P.H. and Overmars, K.P., 2009. Combining top-down and bottom-up dynamics in  
594 land use modeling: exploring the future of abandoned farmlands in Europe with the DynaCLUE  
595 model. *Landscape ecology*, 24, pp.1167-1181.

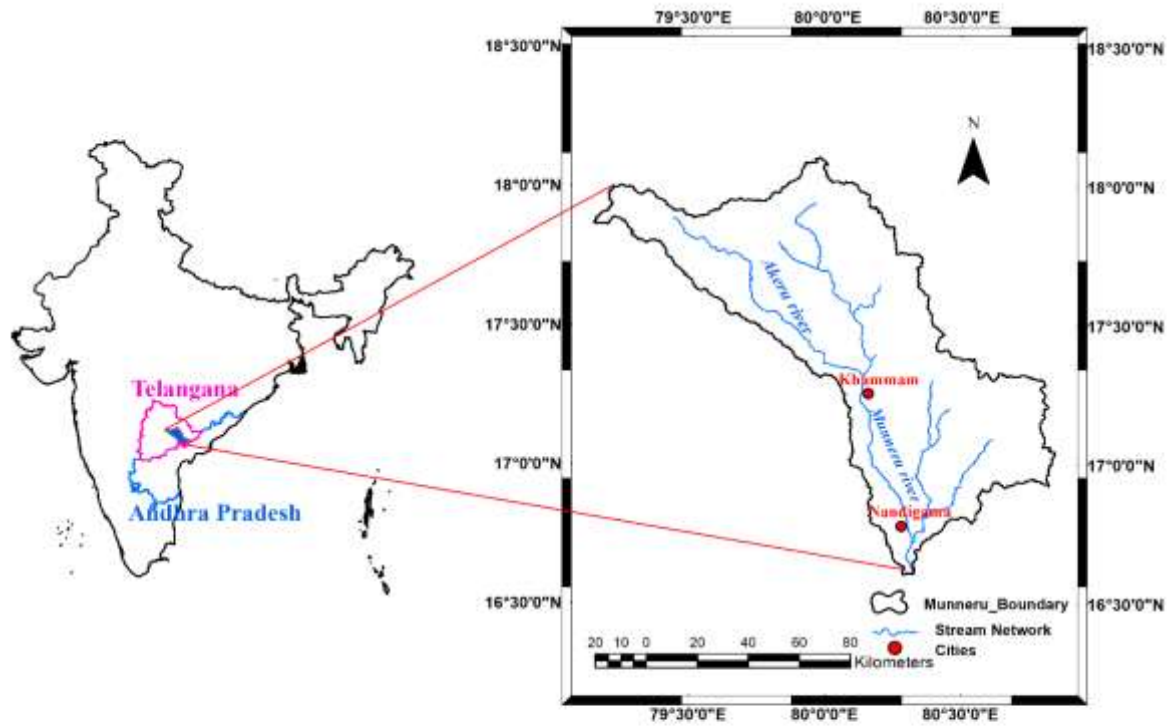
596 Verburg, P., 2010. The CLUE Modelling Framework user manual.  
597 (<http://environmentalgeography.nl/files/data/public/cluemanual>) (last accessed on  
598 30.01.2023).

599 Waiyasusri, K. and Chotpantararat, S., 2022. Spatial evolution of coastal tourist city using the  
600 DynaCLUE model in Koh Chang of Thailand during 1990–2050. *ISPRS International Journal  
601 of Geo-Information*, 11(1), p.49.

602 Wang, Q., Xu, Y., Wang, Y., Zhang, Y., Xiang, J., Xu, Y. and Wang, J., 2020. Individual and  
603 combined impacts of future land-use and climate conditions on extreme hydrological events in  
604 a representative basin of the Yangtze River Delta, China. *Atmospheric Research*, 236,  
605 p.104805.

606 Yao, S., Chen, C., He, M., Cui, Z., Mo, K., Pang, R. and Chen, Q., 2023. Land use as an  
607 important indicator for water quality prediction in a region under rapid urbanization. *Ecological*  
608 *Indicators*, 146, p.109768.

609

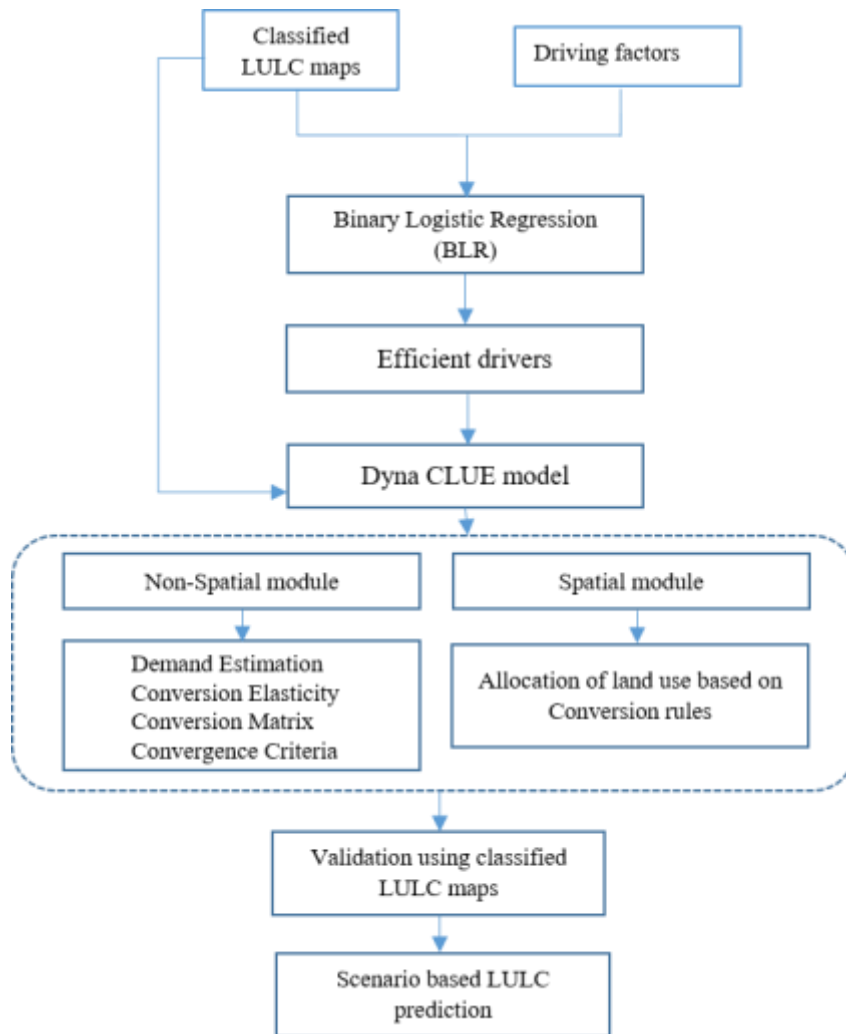


610  
 611  
 612  
 613  
 614  
 615  
 616  
 617  
 618  
 619  
 620  
 621  
 622  
 623  
 624  
 625  
 626

**Figure 1.** Munneru basin location map

627

628



629

630

631

**Figure 2.** Methodology flowchart of the present study

632

633

634

635

636

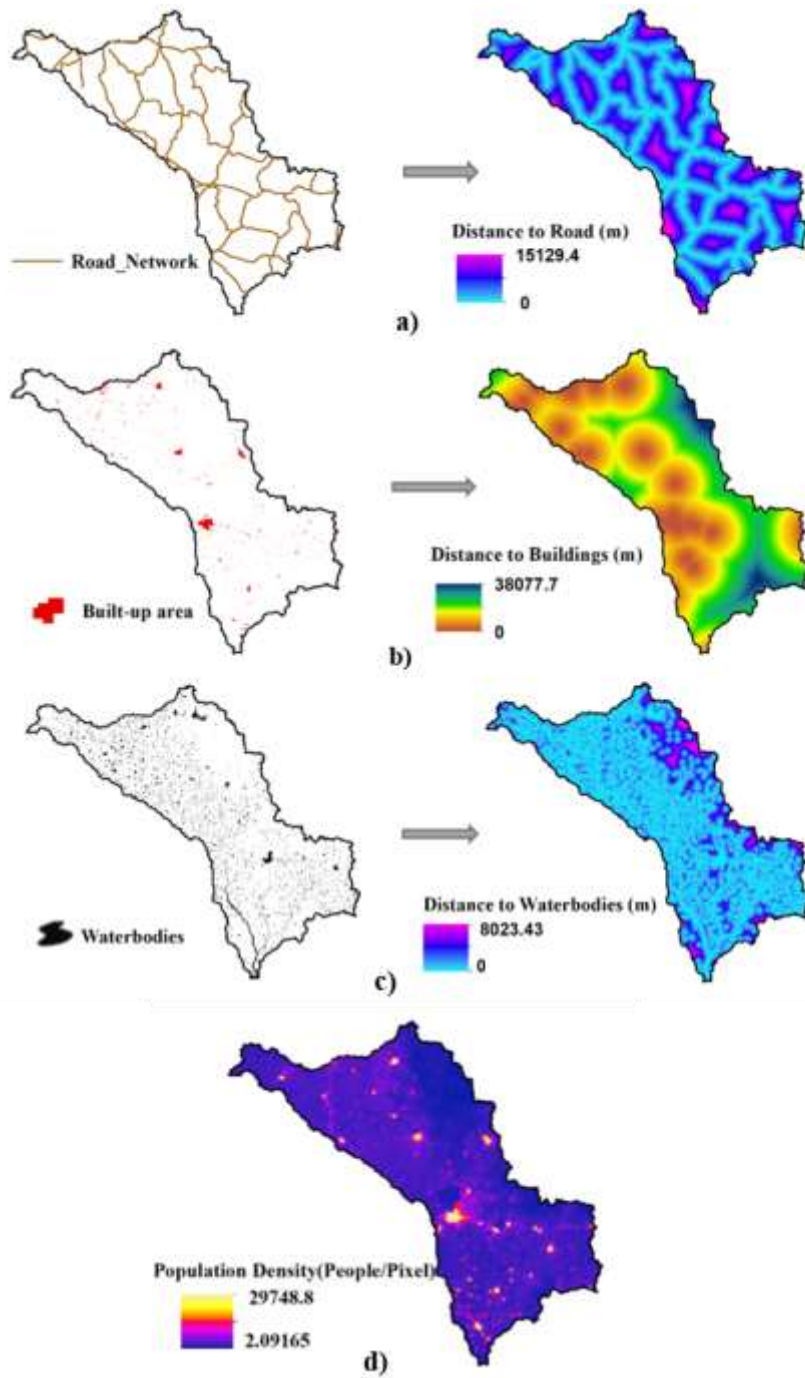
637

638

639

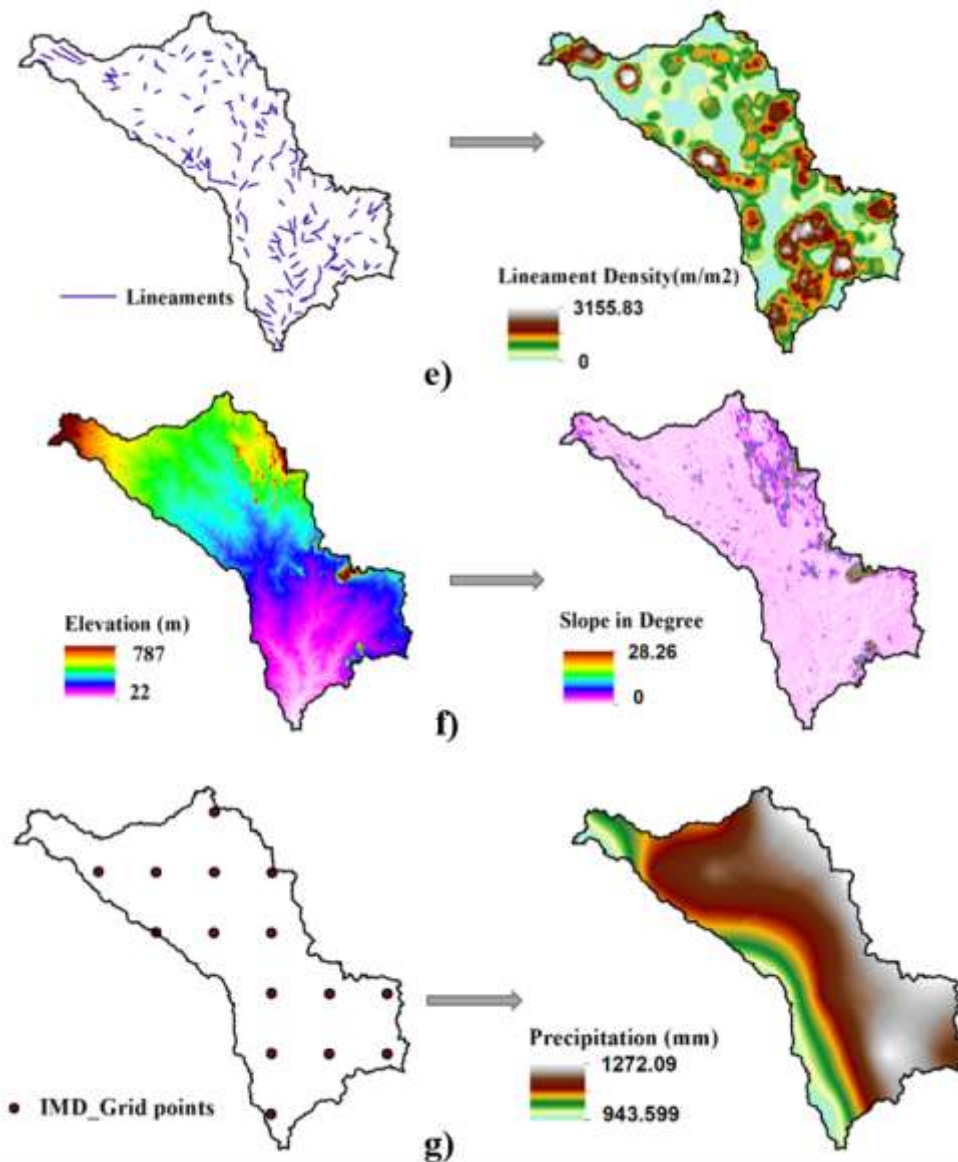
640

641



642  
 643  
 644  
 645  
 646  
 647  
 648  
 649  
 650

**Figure 3.** Driving factors considered for LULC projection (a) Distance to Road (b) Distance to Buildings (c) Distance to Waterbodies (d) Population Density



651

652 **Figure 4.** Driving factors considered for LULC projection (e) Lineament Density (f) Slope

653

(g) Precipitation

654

655

656

657

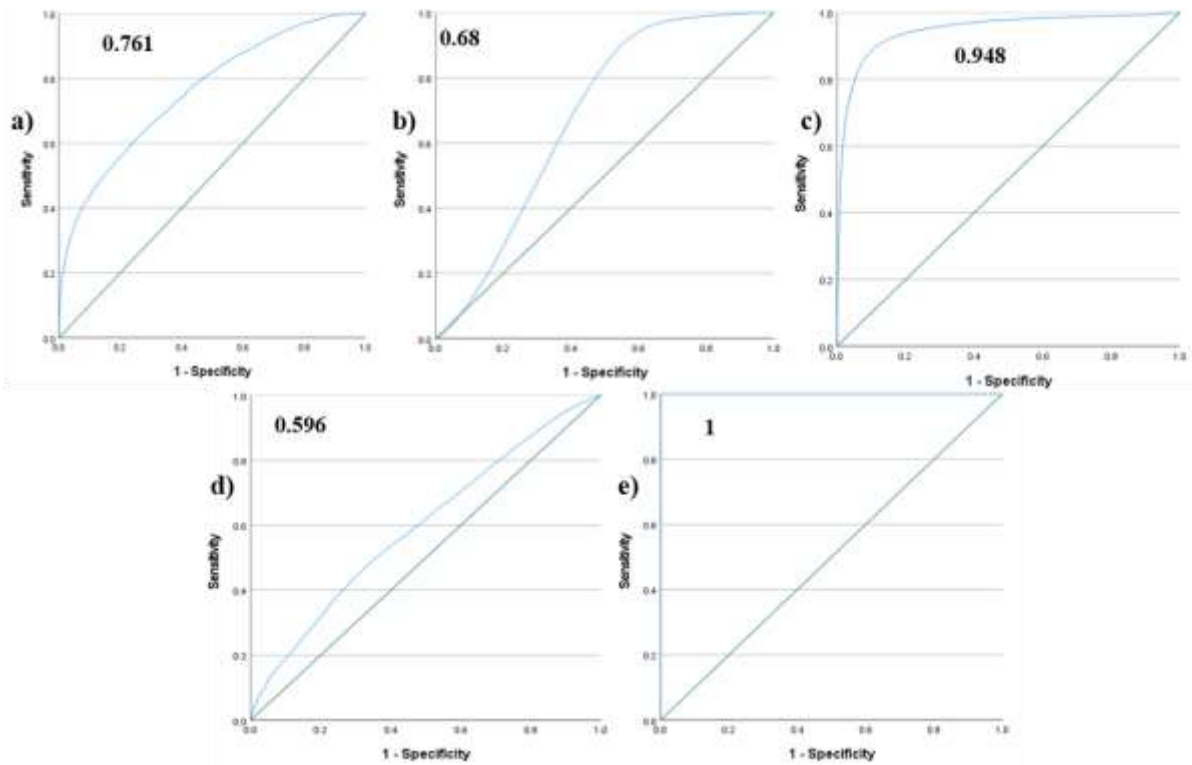
658

659

660

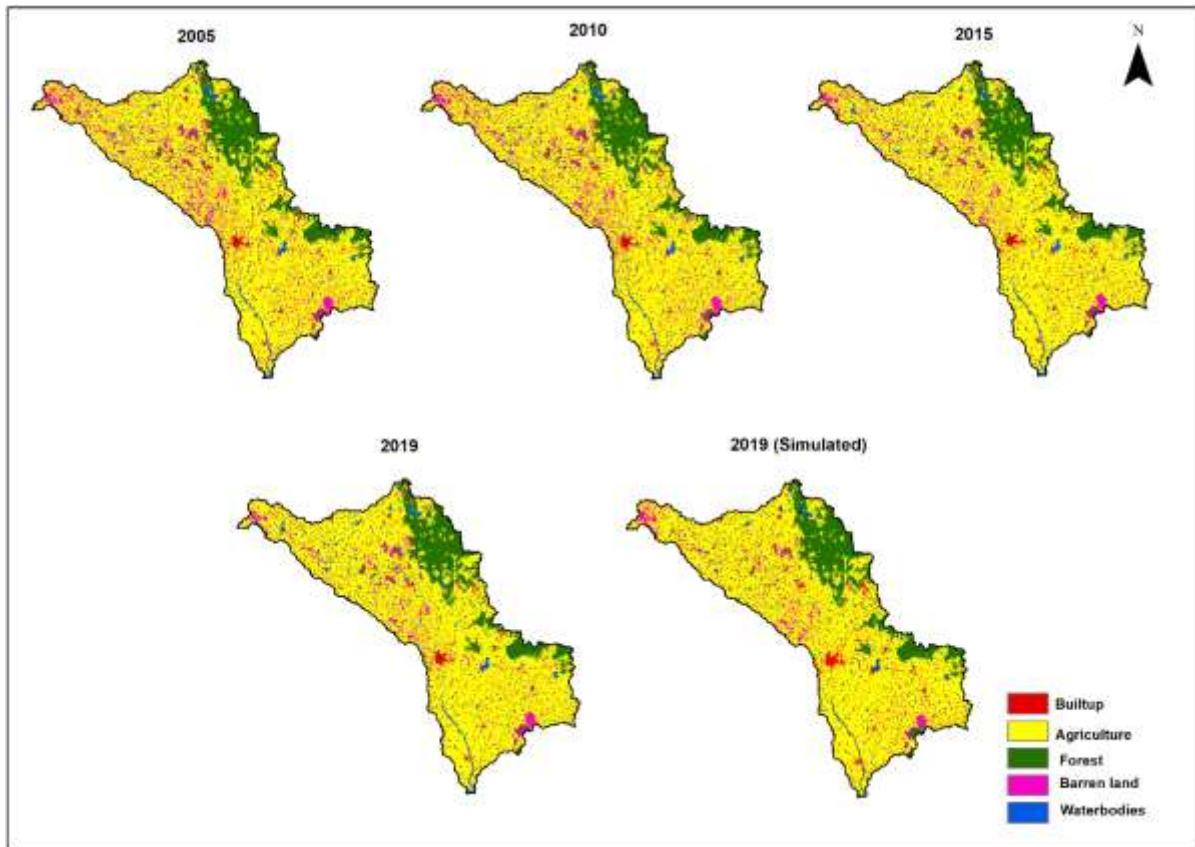
661

662



663  
 664  
 665  
 666  
 667  
 668  
 669  
 670  
 671  
 672  
 673  
 674  
 675  
 676  
 677  
 678  
 679  
 680  
 681  
 682

**Figure 5.** ROC curve for LULC classes a) Built-up b) Agriculture c) Forest d) Barren land e) Waterbodies



683

684 **Figure 6.** Classified LULC maps for 2005, 2010, 2015, 2019 years and the simulated (2019)

685

LULC map

686

687

688

689

690

691

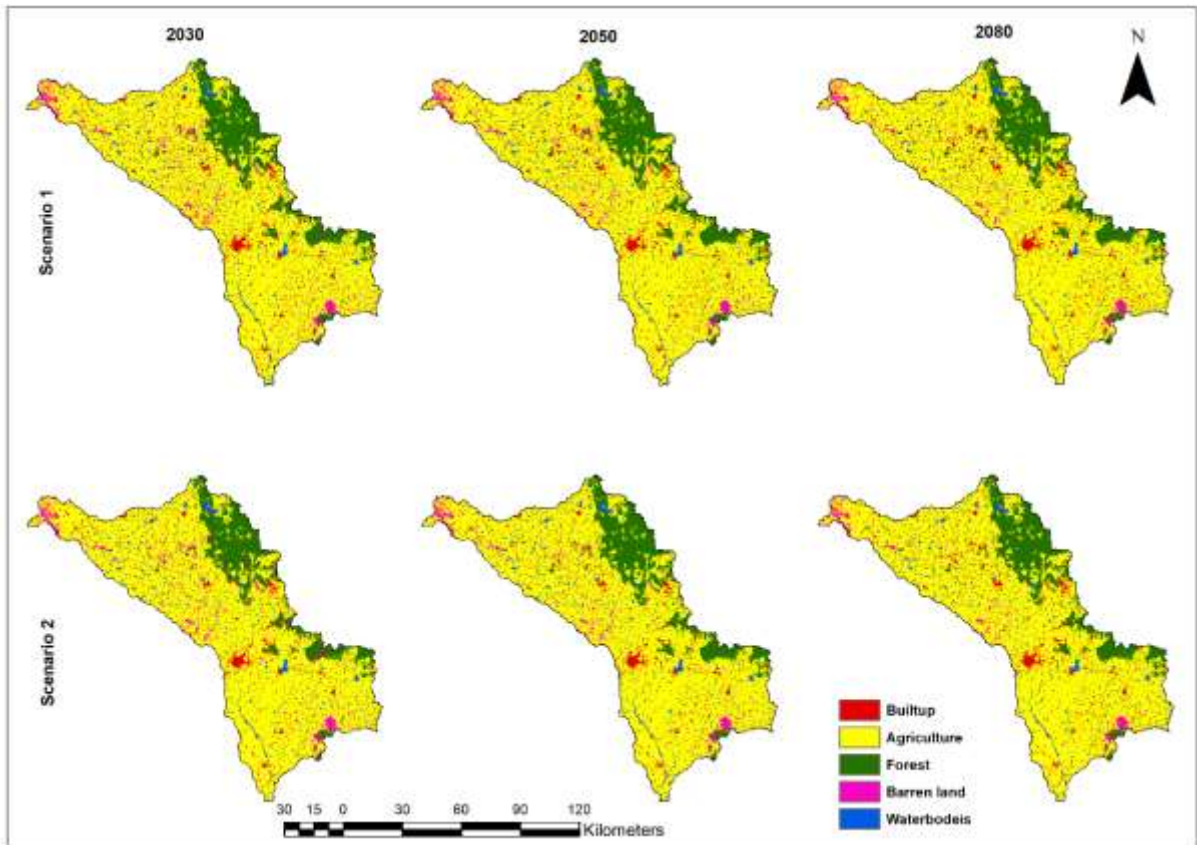
692

693

694

695

696



697

698 **Figure 7.** Predicted LULC's for 2030, 2050 and 2080 years with Scenario 1 and Scenario 2

699

700

701

702

703

704

705

706

707

708

709

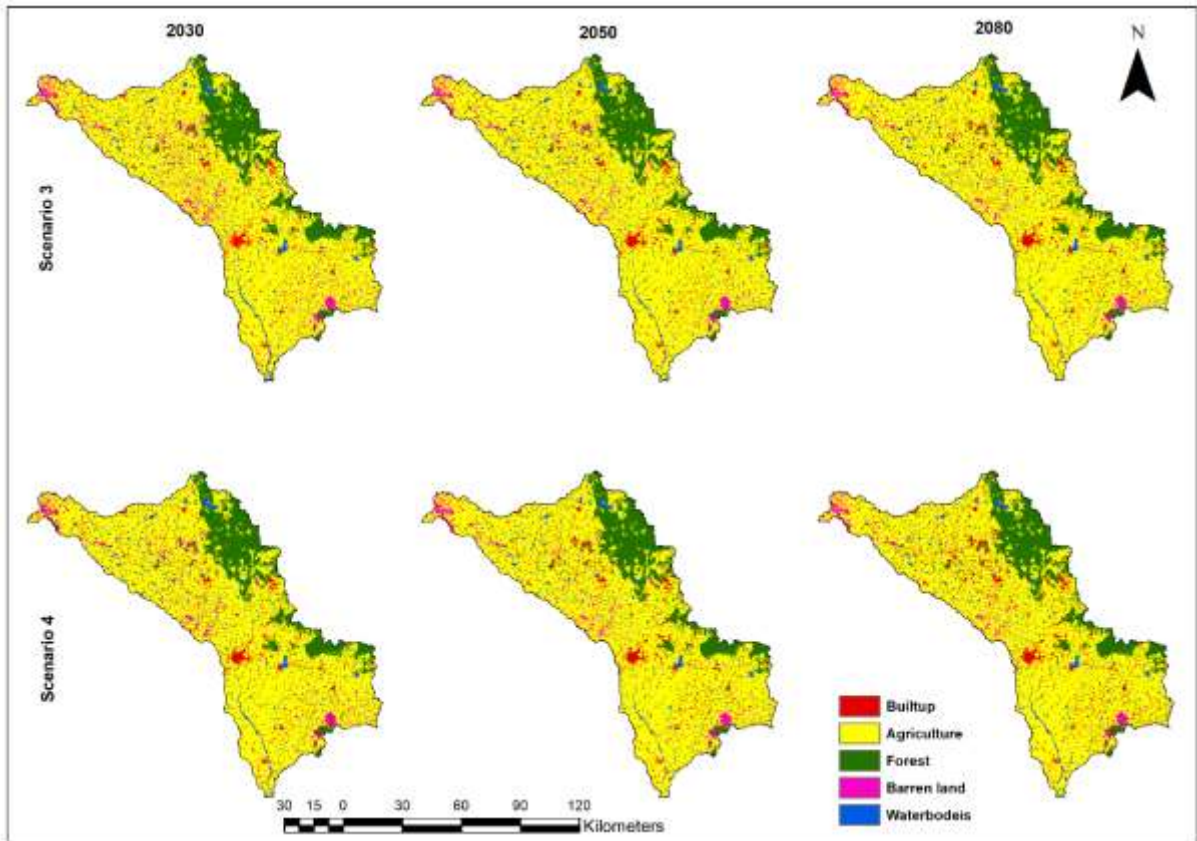
710

711

712

713

714



715

716

717 **Figure 8.** Predicted LULC's for 2030, 2050 and 2080 years with Scenario 3 and Scenario 4

718

719

720

721

722

723

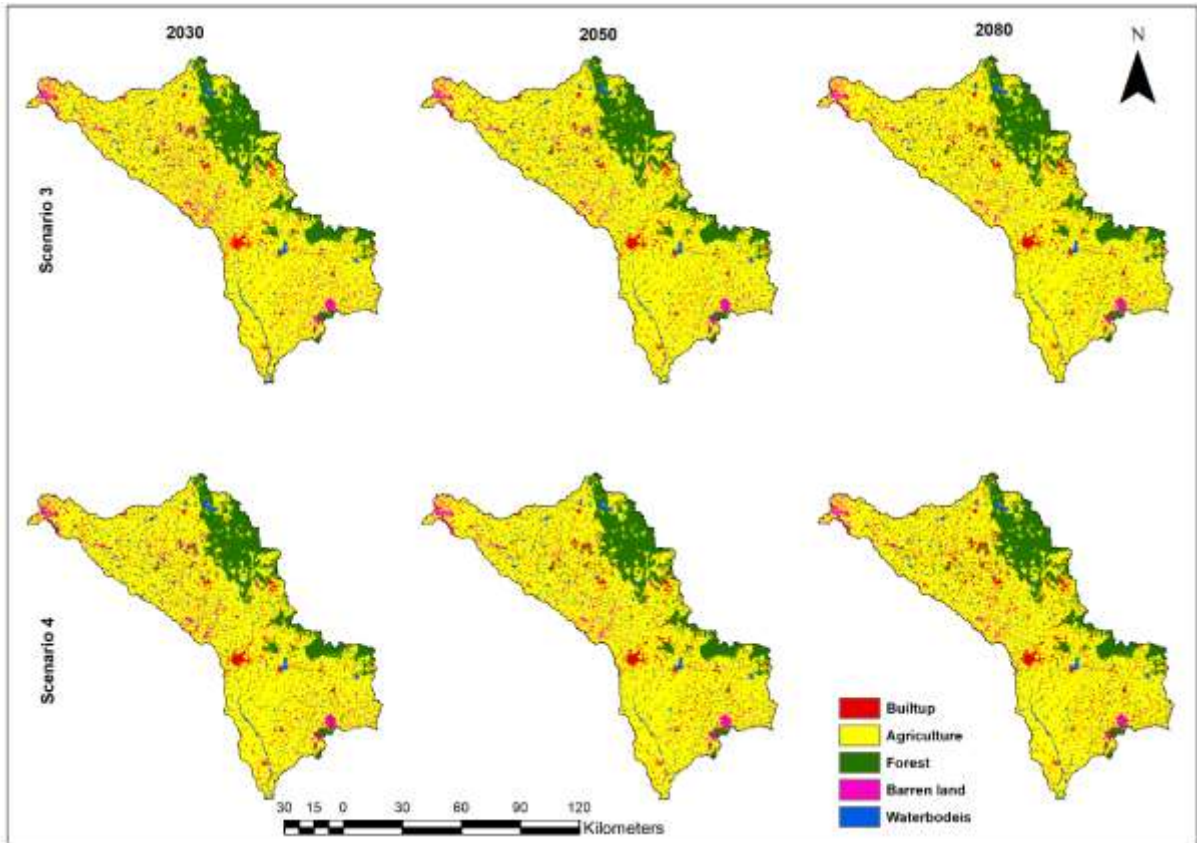
724

725

726

727

728



729

730 **Figure 9.** Predicted LULC's for 2030, 2050 and 2080 years with Scenario 5 and Scenario 6

731

732

733

734

735

736

737

738

739

740

741

742

743

744

745

746

747 **Table 1.** Scenarios considered for projection of future LULC maps

Scenario	Description
Scenario 1	Similar Change as in the period 2005-2015
Scenario 2	Similar Change as in the period 2010-2019
Scenario 3	Increase in Built-up area (2 Km <sup>2</sup> per year) with unchanged forest area
Scenario 4	Increase in Built-up area (6 Km <sup>2</sup> per year) with unchanged forest area
Scenario 5	Increase in Built-up area and agricultural land (2 Km <sup>2</sup> per year and 10 Km <sup>2</sup> per year) with change in the forest area
Scenario 6	Increase in Built-up area and agricultural land (6 Km <sup>2</sup> per year and 20 Km <sup>2</sup> per year) with change in the forest area

748

749 **Table 2.** Binary logistic regression analysis for input drivers

Driving Variables	$\beta$ - coefficient and its exponential	LULC Type				
		Built-up	Agriculture	Forest	Barren land	Waterbodies
Distance to Buildings	$\beta$	-0.0000175	-0.0000051	-	0.0000173	-0.000661
	Exp( $\beta$ )	0.999982	0.999995	0.9999505	1.0000173	0.99933
Precipitation	$\beta$	-0.0011895	0.0029684	0.0210682	-0.0053235	0.00018
	Exp( $\beta$ )	0.998811	0.997036	1.0212917	0.9946906	1.00018
Lineament Density	$\beta$	-	0.038473	-	-0.000173	0.000273
	Exp( $\beta$ )	-	1.03922	-	0.9998	1.000273
Population density	$\beta$	0.0009886	-0.0002526	-	-	-0.012298
	Exp( $\beta$ )	1.000989	0.9997475	0.9905322	-	0.9877
Distance to road	$\beta$	0.0000805	-0.0000158	-	-0.0000143	-
	Exp( $\beta$ )	0.999919	0.9999843	0.9999909	0.9999857	-
Slope	$\beta$	-0.1655022	-0.6310085	0.3173325	-0.0837166	-0.048153
	Exp( $\beta$ )	0.847468	0.532055	1.3734592	0.9999383	0.95298
Distance to waterbodies	$\beta$	-0.0002498	-0.0002498	0.0008879	-0.0000617	-0.1274863
	Exp( $\beta$ )	0.99975	0.9997503	1.0008883	36.0041096	0.88

750

751

752

753

754

755 **Table 3.** Area wise distribution of classified LULC maps

<b>LULC/ Area in ha</b>	<b>2005</b>	<b>2010</b>	<b>2015</b>	<b>2019</b>	<b>2019 (Simulated)</b>
Built-up	31513.53	37152.84	37588.03	38020.95	37565.82
Agriculture	711774.26	716209.59	737938.14	747823.42	737793.26
Forest	141596.25	141596.25	141032.96	141006.20	140865.60
Barren land	98673.53	88584.11	69013.54	58724.23	69024.40
Waterbodies	55642.43	55657.21	53627.33	53625.20	53781.20

756

757 **Table 4.** Percentage of LULC types in the study area for the Base year (2019) and for the years  
758 2030, 2050 and 2080 under different scenarios

<b>Year</b>	<b>Scenario</b>	<b>Change in LULC (%)</b>				
		<b>Built-up</b>	<b>Agricultural Land</b>	<b>Forest Land</b>	<b>Barren Land</b>	<b>Waterbodies</b>
<b>2019</b>	Base	3.7	71.9	13.6	5.6	5.2
<b>2030</b>	Scenario 1	4.2	73.6	13.3	3.9	5.0
	Scenario 2	4.1	74.9	12.5	3.7	4.8
	Scenario 3	3.9	72.4	13.7	4.7	5.3
	Scenario 4	4.3	73.1	13.6	3.9	5.0
	Scenario 5	3.9	73.4	13.2	4.5	5.1
	Scenario 6	4.4	74.1	12.6	3.9	5.0
<b>2050</b>	Scenario 1	5.2	73.8	13.5	2.8	4.8
	Scenario 2	4.4	74.4	13.6	2.6	4.9
	Scenario 3	4.8	73.6	13.5	3.1	5.0
	Scenario 4	5.8	73.2	13.5	2.7	4.8
	Scenario 5	4.8	73.7	13.2	3.4	4.8
	Scenario 6	5.8	74.7	12.9	1.8	4.8
<b>2080</b>	Scenario 1	5.9	74.2	13.3	1.9	4.7
	Scenario 2	5.3	74.9	13.2	1.8	4.8
	Scenario 3	5.5	73.7	13.5	2.4	4.9
	Scenario 4	7.0	72.6	13.5	1.9	4.9
	Scenario 5	5.5	75.2	12.1	2.3	4.9
	Scenario 6	7.0	76.0	10.8	1.4	4.8

759

760

761

762

763

764

765

766